EUROPEAN FUSION DEVELOPMENT AGREEMENT

EFDA–JET–PR(04)64

J. Weiland, E. Asp, X. Garbet, P. Mantica, V. Parail, P. Thomas,
W. Suttrop, T. Tala and JET EFDA contributors

Effects of Temperature Ratio on JET Transport in Hot Ion and Hot Electron Regimes

Effects of Temperature Ratio on JET Transport in Hot Ion and Hot Electron Regimes

J. Weiland[1], E. Asp[2], X. Garbet[2], P. Mantica[3], V. Parail[4], P. Thomas[2], W. Suttrop[5], T. Tala[6] and JET EFDA contributors*

[1]*Chalmers University of Technology and EURATOM-VR Association, Gothenburg, Sweden*
[2]*Association EURATOM-CEA sur la Fusion, CEA Cadarache, France*
[3]*Istituto di Fisica del Plasma CNR-EURATOM, Milano, Italy*
[4]*EFDA-JET, Culham Science Centre, Abingdon, UK*
[5]*Max-Planck Institut fuer Plasmaphysik, Garching, Germany*
[6]*Association EURATOM-TEKES, VTT Processes, Helsinki, Finland*
** See annex of J. Pamela et al, "Overview of Recent JET Results and Future Perspectives", Fusion Energy 2002 (Proc.19 th IAEA Fusion Energy Conference, Lyon (2002).*

Preprint of Paper to be submitted for publication in
Plasma Physics and Controlled Fusion

ABSTRACT

Two series of JET shots, one on hot ion shots and one on hot electron shots, have been analysed in order to improve the understanding of how the temperature ratio T_e/T_i influences the performance. Comparisons are also made with ITER simulations which are in the hot electron regime. The temperature ratio has been varied between different shots, in partly interpretative simulations of one shot and locally. The effect of the variation of the temperature ratio depends strongly on how it is done but can also be different in different types of shots. In general, however, an increased electron heating deteriorates confinement rather strongly. This is the situation for increasing the alpha power in ITER. ITER simulations show, however, that the effect is not dramatic.

1. INTRODUCTION

The favourable aspects of the hot ion regime for confinement have been well known since the initial success of neutral beam heating [1]. The basic reason for the present interest in effects of the temperature ratio T_e/T_i on tokamak transport is the fact that most present day high performance shots have strong ion heating while a burning machine, like ITER, will have most of the heating on electrons. In order to try to understand the importance of the temperature ratio, two series of JET shots, one in the hot ion regime [2] and one in the hot electron regime [3] have been analysed by predictive transport simulations. The hot electron regime was analysed in [4]. In the present work the main focus will be on the hot ion regime.

The transport model used is theWeiland drift wave model [5]. This model includes the Ion Temperature Gradient (ITG) mode, the Trapped Electron (TE) mode, the impurity ITG mode, the Kinetic Ballooning (KB) mode and the MagnetoHydroDynamic (MHD) ballooning mode. The ITG mode includes both slab and curvature (toroidal) drive and the TE mode can be driven by both the density gradient (ubiquitous mode) and by the Electron Temperature Gradient (ETG) (compressional TE mode). The compressional TE mode is usually the most important TE mode in the bulk of H-mode plasmas due to the flat density gradients there. It is essentially symmetric to the ITG mode and thus has a dispersion relation similar to that of the ETG mode which is, however, not included. Its threshold is not expected to be reached by the gradients occurring in the experiments studied here. The KB mode is electromagnetic. Its growth rate increases with β and it connects to the MHD ballooning mode in the MHD unstable regime. It is usually only important near the axis. The transport coefficients include a full transport matrix including possibilities for fluxes that increase gradients (pinches). The present work focuses on JET shots but also makes comparisons with D-III-D [6] and AUG [7]. These relate to modulations in heating as also studied in JET [8]. Finally, comparisons with ITER simulations are also made [9]. The simulations in this work were made with the recently upgraded version of our transport model [10].

2. BRIEF OVERVIEW OF JET PULSES

Here we are mainly going to show results from simulations of hot ion H-modes. Comparisons will, however, be made with a JET hot electron H-mode, Pulse No: 52096.

The electron temperature was measured from electron cyclotron radiation while the ion temperature was measured by charge exchange spectroscopy. The electron density was measured by Thomson scattering. The error bars are typically around 10% on electron temperature and density and about 15% on ion temperature.

Here the % alpha power is on the auxiliary electron heating. The peaking factor (Peak) is defined as the ratio of central density and density at half radius. The toroidal magnetic field was around 3.5T for all shots and the plasma current around 2.5MA.

Comparison was made with the hot electron H-mode shot 52096 [3, 4]. Here the diagnostics was the same except for electron temperature which was here also measured by Thomson scattering.

3. BASIS OF ITG AND TE MODE SCALINGS

In the flat density tokamak core the ITG and TE modes are basically resonant modes associated with fluid resonances. In this regime they decouple and are in the simplest toroidal case described by quadratic dispersion relations. Including also the dilution on the ITG due to electron trapping (fraction f_t), we use the notations: ω_{*j} and ω_{Dj} are the diamagnetic and magnetic drift frequencies where j indicates particle species (as also in other quantities). $L_j = -j/(\partial j/\partial r)$ is the scale length of profile quantity j and $\eta_j = L_n/L_{Tj}$ is the ratio of density to temperature scale lengths of quantity j. Furthermore the subindex 'th' indicates threshold. Now also introducing the trapped fraction f_t we have:

3.1. ITG (LOCAL LIMIT)

$$\omega = \omega_r + \sqrt{\omega_{*e}\omega_{*i}(\eta_i - \eta_{ith})} \qquad (1a)$$

$$\omega_r = \frac{1}{2}\omega_{*e}\left[1 - \varepsilon_n\left(1 + \frac{10}{3\tau}\right)\right] \qquad \tau = \frac{T_e}{T_i}, \quad \varepsilon_n = \frac{\omega_{De}}{\omega_{*e}}. \qquad (1b)$$

The local ITG threshold without finite Larmor radius (FLR) effects is:

$$\frac{R}{L_{ti}} = \frac{4}{3\varepsilon_n} + \frac{20}{9\tau}(1 - f_t) - \frac{\tau}{(1 - f_t)\varepsilon_n} + \frac{\tau}{2(1 - f_t)} + \frac{\tau}{2\varepsilon_n^2(1 - f_t)}. \qquad (1c)$$

The nonlocal ITG threshold is:

$$\frac{R}{L_{ti}} = \frac{4}{3\varepsilon_n} + \frac{20}{9\tau}(1 - f_t). \qquad (1d)$$

Here the nonlocal threshold was obtained by solving the linear eigenvalue equation analytically in the strong ballooning limit. This means that parallel ion motion, and thus the slab ITG, is included. The local threshold is obtained when parallel ion motion can be neglected. It follows from the strong ballooning case if we let the safety factor q go to infinity. In this limit we have only the toroidal drive for the ITG mode. This is shown by the property of (1c) that the threshold expressed in η_i (after multiplication of (1c) by ε_n) approaches infinity when ε_n tends to zero.

3.2. TE MODE

$$\omega = \omega_r + \sqrt{-\Gamma \omega_{*e} \omega_{De} (\eta_e - \eta_{eth})} \tag{2a}$$

$$\omega_r = -\frac{1}{2}\omega_{*e}\left[\Gamma - \varepsilon_n\left(\Gamma + \frac{10}{3}\right)\right], \qquad \Gamma = \frac{f_t}{1 - f_t}. \tag{2b}$$

The threshold is:

$$\frac{R}{L_{Te}} = \frac{4}{3\varepsilon_n} + \frac{20}{9\Gamma} + \frac{\Gamma}{2}\left(1 - \frac{1}{\varepsilon_n}^2\right). \tag{2c}$$

We note the trend for the ITG and TE modes to propagate in different directions. The phase velocities have equal magnitudes but opposite signs when ft = 0.5 and f = 1 if FLR effects are ignored.

It is interesting to note the (quasi-) symmetry in phase velocities while the temperature behaviour is asymmetric. The ITG mode is driven by the root of the product of ion and electron drifts while the TE mode is driven by purely electron drifts. This ideal form of the TE mode does not depend on the ion temperature at all. (We note the difference to the ubiquitous mode which is actually due to a coupling between the present modes.) We also note that the threshold of the ITG mode increases in the hot ion regime while that of the TE mode is independent of temperature. The transport code which we will use, of course, includes all couplings and intermediate states between the 'ideal' modes considered above. We, however, expect that confinement will deteriorate when we increase T_e while an increase in T_i has two counteracting effects: both the driving term and the threshold will increase.

We have given here both the local and the nonlocal ITG thresholds. The nonlocal threshold is actually the threshold of the slab ITG mode while the local threshold gives the onset of the toroidal ITG mode. The local threshold is always larger than or equal to the nonlocal threshold. Since the toroidal ITG mode is stronger than the slab ITG mode, we have a kind of two-step process. When we increase the temperature gradient we first get the slab ITG mode and then the toroidal ITG mode.

4. SIMULATIONS

The simulations were predictive for both temperatures and electron density. The impurity density was kept as a fixed fraction of the electron density and the ion density was then obtained from quasineutrality. The simulations were made for one time slice of the experiment, i.e. with fixed sources, outer boundaries and MHD equilibrium. The inner boundary, at 10% of the minor radius, had a flat profile while the outer boundary, at 90% of the small radius, had a fixed value. An additional diffusivity of $0.2 m^2 s^{-1}$ was added between 10% and 20% of the small radius for electron temperature and density simulation. This is because the drift waves sometimes become stable in this region. For the rotation, a radial electric field is obtained from radial pressure balance, including neoclassical effects and a toroidal velocity taken from experiment. This is a full paper version of the EPS paper P1 160. The simulations in this paper are all made by the new version [10] of the model with varying correlation length. This is the reason for minor differences.

The JET shots we study here [2] are from the Tritium campaign. Recent JET shots using ICRH with minority heating [3] have obtained T_e/T_i of about 2. These shots do not have the very good confinement of the hot ion regime but are still not far from typical scaling laws.

Although it is well known that the hot ion regime gives reduced transport in ITG models, it has usually been difficult to recover the very high central ion temperature in transport simulations using ITG transport. In the present simulations we have succeeded rather well in most cases. The confinement has been improved by rotation and finite beta effects. The decrease of ion temperature with increased electron heating seen on D-III-D andAUG has been recovered qualitatively by artificially increasing the NBI electron heating in the simulations of JET shots. Transport barriers were obtained by artificially increasing the ion heating also without rotation. Finite beta effects tend to contribute to this by giving an ion heat pinch.

The radial profiles of T_i and T_e from experiment [2] and simulation for a typical hot ion pulse (Pulse No: 42856) are shown in Fig. 1. In this shot the auxiliary heating was only a neutral beam with 7.3MW on ions and 2.3MW on electrons. This was a DT shot with alpha power 0.31MW on electrons. A simulation of another hot ion JET shot with less peaked density is shown in Fig. 2.

The peaking factors are seen in Table 1. Although Pulse No: 42847 has slightly more heating, Pulse No: 42856 has somewhat higher temperatures. Note that the scales on the *y*-axis do not start at zero. For the density in Pulse No: 42847 it starts at 2.6×10^{19}. Thus the maximum error in the simulation is 13%. Although the difference in peaking is not within the accuracy of the simulations, the trends in the simulations are the same as in the experiments.

We have also simulated the DD reference Pulse No: 40365. The simulation was quite successful but behaved very similarly to those of the DT shots. One noticeable difference was, however, that the ion temperature was slightly higher without alpha heating. This was because of a feedback loop, involving the ITG threshold, which will be discussed later.

5. THRESHOLDS AND STIFFNESS

As seen from equation (1*b*), the ITG threshold depends on the temperature ratio while the TE threshold does not, as seen from equation (2*c*). This is why the hot ion regime is favourable for ion energy transport. Actually the ion energy transport has a maximum as a function of T_e/T_i when the ion temperature is varied and the electron temperature is kept fixed. This is a property directly related to the ideal, decoupled modes as described by equations (1) and (2) but this property also remains in the full, coupled system as we will soon see. As shown by Fig. 2, however, both ITG and TE thresholds have a stronger impact on the temperature profiles in the hot ion regime than in the hot electron regime. Although we plot the thresholds of the ideal modes, the temperature profiles are controlled by the coupled modes. This is why the electron temperature stays closer to its threshold in the hot ion case. The T_e mode is actually stiffer in the hot ion regime than at comparable temperatures. Also, the ITG mode stays closer to threshold. However, an increased ion heating leads to a higher ITG threshold and, accordingly, to reduced transport. Thus, an increased ion

heating tends to give a comparatively large increase in the ion temperature and sometimes even an ion ITB can result.

As seen in Fig. 3, the radial shapes of thresholds of ITG and TE modes and the corresponding experimental gradient profiles of T_i and T_e are very different for hot ion and hot electron shots. In the hot ion regime, profiles tend to follow thresholds all the way out to the edge. This is particularly clear for the ITG mode. We have here plotted the local ITG threshold which is similar to the TE threshold. It gives the threshold of the toroidal ITG mode which has the larger growth rate. We can see that the threshold increases in the hot ion regime for large ε_n. This is particularly obvious for the nonlocal threshold. However, here all the terms are contributing. It is important to remember that while the thresholds are those of the ideal modes, the temperature profiles are caused by the full model containing all the couplings between the modes. This is why there is a difference at all for the TE mode since the ideal mode does not depend on the temperature ratio. The thresholds of ITG and TE modes are not directly comparable since ε_n is also different. In general, the thresholds seem to play a more important role in the hot ion regime since the temperature profiles are closer to threshold.

Tests were made by artificially increasing the NBI electron heating with a space independent factor in the simulations. By doubling the electron heating, the central electron temperature increased by 10% while the central ion temperature decreased by 9%. When the electron heating was multiplied by 4, the central T_e increased by 15% while the central T_i decreased by 28%. This shows that the electron channel is very stiff while the ion temperature is reduced for increased electron heating. Such qualitative trends have been seen experimentally on D-III-D [5] andAUG[6]. In the simulations the reason for this is a reduction of the threshold of the ITG mode when T_e/T_i is increased.

When the ion heating was increased artificially in the simulations of the hot ion regime, the ion temperature increased strongly and eventually a transport barrier was formed. The simulations in the hot ion regime were very sensitive due to the appearance of transport feedback loops. One such loop is active in connection with an increase of electron heating. Here the increased T_e leads to increased T_e/T_i which decreases the ITG threshold. This leads to a reduction of T_i and a further increase in T_e/T_i. The feedback is terminated when the parts of the threshold (1c) that grow with f become comparable to the term with f in the denominator. The opposite feedback loop gets activated upon a decrease of electron heating. Another feedback loop involves rotation. An increased density gradient gives increased rotation which gives an increased temperature gradient. An increased temperature gradient will, through off-diagonal transport fluxes, reduce the particle transport and the density gradient is increased. Because of this, transport barriers can sometimes also be formed in the simulations when the experiment does not have a barrier. This is because of the strongly nonlinear situation giving a possible bifurcation. Thus, in some cases either the particle transport or the rotation had to be turned off.

In the hot electron regime, good agreement was, in general, obtained with the temperature profiles of the JET shots in this regime [4]. However, strong stiffness was obtained in the simulations when

the electron heating was artificially increased by a factor of 4 or more and we had both ion and electron heating. This could even lead to increasing gradient scale lengths in steady state [4]. At the transition to the latter behaviour, there is a region where the gradient scale length is independent of the heating power. Here the incremental stiffness, in the sense of change in gradient length scale in response to increased heating, is infinite. The conventional stiffness, in terms of transport coefficients, was also high. It was actually about a factor 3 higher than for the experimental case when the electron heating was increased by a factor 5. This was at half radius where the temperature gradient length scales had changed very little. The main reason for the increased stiffness was the increased temperatures (due to the gyro-Bohm scaling of diffusion coeffficients as $T^{1.5}$). No transport barrier could be obtained. Note, however, that perturbative simulations close to experimental profiles with only electron heating indicated mild stiffness [8]. The characteristics of gradient profiles were very different in hot electron and hot ion regimes and the hot ion regime gave good confinement. Nevertheless, replacing ion heating by electron heating can be beneficial. This is due to a kind of dilution effect caused by the fact that only TEs contribute to transport in low beta plasmas.

6. ION HEAT PINCH

A very interesting feature seen in several simulations of hot ion H-modes is the presence of strong off-diagonal or convective ion heat fluxes. In several cases, quite small artificial changes in the simulated profile could give a net ion heat pinch. This pinch turned out to be due to electromagnetic effects. In general we can write the ion effective diffusivity in the form:

$$\chi_i = \frac{1}{\eta_i}\left[\eta_i - \frac{2}{3} - (1 - f_t)\left(\frac{10}{9\tau}\varepsilon_n + \Delta_{em}\right) - \frac{2}{3} f_t \Delta_i\right] \frac{\gamma^3/k_x^2}{(\omega_r - 5\omega_{Di}/3)^2 + \gamma^2}\,. \qquad (3)$$

This result has been obtained by expressing the ion density perturbation in that of free and TEs using quasineutrality. Thus, Δ_i is due to the TE response. The new, electromagnetic part is Δ_{em}, which is the effect of electromagnetic free electrons. It becomes important roughly when $\beta_e \approx s^2/(2q^2)$ and is then comparable with the electrostatic heat pinch. It has components driven by curvature alone as well as a combination of ETG and curvature. Just as for the electrostatic ion heat pinch, the ETG drives an electromagnetic heat pinch if the eigenmode propagates in the ion drift direction. From (3) we immediately observe a significant pinch part, due to electrostatic free electrons, which becomes large in the hot ion regime. In the simple electrostatic case without trapping, there can be no pinch because the ITG mode is stable in this regime. However, TE and KB modes (electromagnetic) can be unstable in this regime and can thus give an ion heat pinch. For the hot ion H modes it is the KB modes that drive the pinch. Figure 4 shows a typical case where we get a pinch by reducing the temperature ratio. In general we can get an electromagnetic ion heat pinch in two basic ways. First, electromagnetic modes (KB modes) can drive an ion heat pinch through the main electrostatic pinch flux in (3). Second, electrostatic modes can drive a heat pinch through em. In general, there can also be combinations of these cases.

We also note the property mentioned above that there is a maximum of χ_i when T_i is varied. This is because the high threshold reduces χ_i in the hot ion regime and the low ion temperature makes the ion curvature drift small in the hot electron regime. The location of this maximum is here at $T_e/T_i \approx 1.8$. It can depend on several parameters, the most obvious of which is ε_n.

7. DISCUSSION

We have seen that transport in hot ion and hot electron regimes can be very different. Although the hot electron regime is more ITER relevant, it is important to understand both the hot ion and hot electron regimes and in particular why the transport is different. As we have seen, several interesting phenomena take place in the hot ion regime. In particular, the system can be very sensitive to small perturbations due to transport feedback loops. Such feedback loops may also lead to the formation of transport barriers. Electromagnetic effects have turned out to be important for the shots studied here. They reduce transport and can even lead to an ion heat pinch. Also elongation becomes important in this case. The temperature ratios in the hot electron JET shots were similar to those obtained in ITER simulations [9] using the same transport model. This gives some more confidence in the ITER predictions which gave fusion $Q = 9$ for the reference design when the density profile was frozen.

ACKNOWLEDGEMENTS

The authors are grateful to Francois Ryter and Adriano Manini for comments and to Annika Eriksson for help with the graphs.

REFERENCES

[1]. J.F.Clarke 1980 *Nucl. Fusion* **20** 563

[2]. P.R. Thomas *et al* 1998 *Phys. Rev. Lett.* **80** 5548

[3]. W. Suttrop *et al* 2001 *Proc. 28th EPS Conf. on Controlled Fusion and Plasma Physics (Funchal, Madeira)* (Mulhouse: European Physical Society) P3.016

[4]. E. Asp *et al* 2005 *Plasma Phys. Control. Fusion* **47**, 505

[5]. J. Weiland 2000 *Collective Modes in Inhomogeneous Plasmas, Kinetic and Advanced Fluid Theory* (Bristol: Institute of Physics Publishing)

[6]. C.C. Petty, M.R. Wade, J.E. Kinsey, R.J. Groebner, T.C. Luce and G.M. Staebler 1999 *Phys. Rev. Lett.* **83** 3661

[7]. A. Manini *et al* 2004 *Plasma Phys. Control. Fusion* **46** 1723

[8]. P. Mantica *et al* 2004 *Proc. 31st EPS Conf. on Controlled Fusion and Plasma Physics (London 2004)* vol 28G, (Mulhouse: European Physical Society) Paper P1.153

[9]. J. Weiland 2001 *Proc. 28th EPS Conf. on Controlled Fusion and Plasma Physics (Funchal, Madeira 2001)* (Mulhouse: European Physical Society) Paper P2.039

[10]. J. Weiland and I. Holod 2005 *Phys. Plasmas* **12** 012505-1

Table 1: Summary of hot ion JET shots.

Pulse No:	T_e/T_i	n_e	P_i	P_e	T_i	T_e
40365	0.58	3.59	6.79	1.69	13.6	7.93
42840	0.58	3.10	7.05	2.62	17.36	10.1
42847	0.63	3.15	7.24	2.81	15.4	9.72
42856	0.65	3.24	7.27	2.27	16.2	10.5
42870	0.55	3.13	6.60	2.26	14.3	7.89
43011	0.72	3.13	6.67	2.95	14.2	10.2

Pulse No:	β%	P_{tot}MW	P_a%el	Peak	Main ion	%T
40365	2.9	10.4	0	1.44	DD	0
42840	2.8	9.7	26	1.57	DT	50
42847	2.2	10.0	14	1.30	DT	50
42856	2.6	9.6	14	1.42	DT	50
42870	2.2	8.9	18	1.44	DT	50

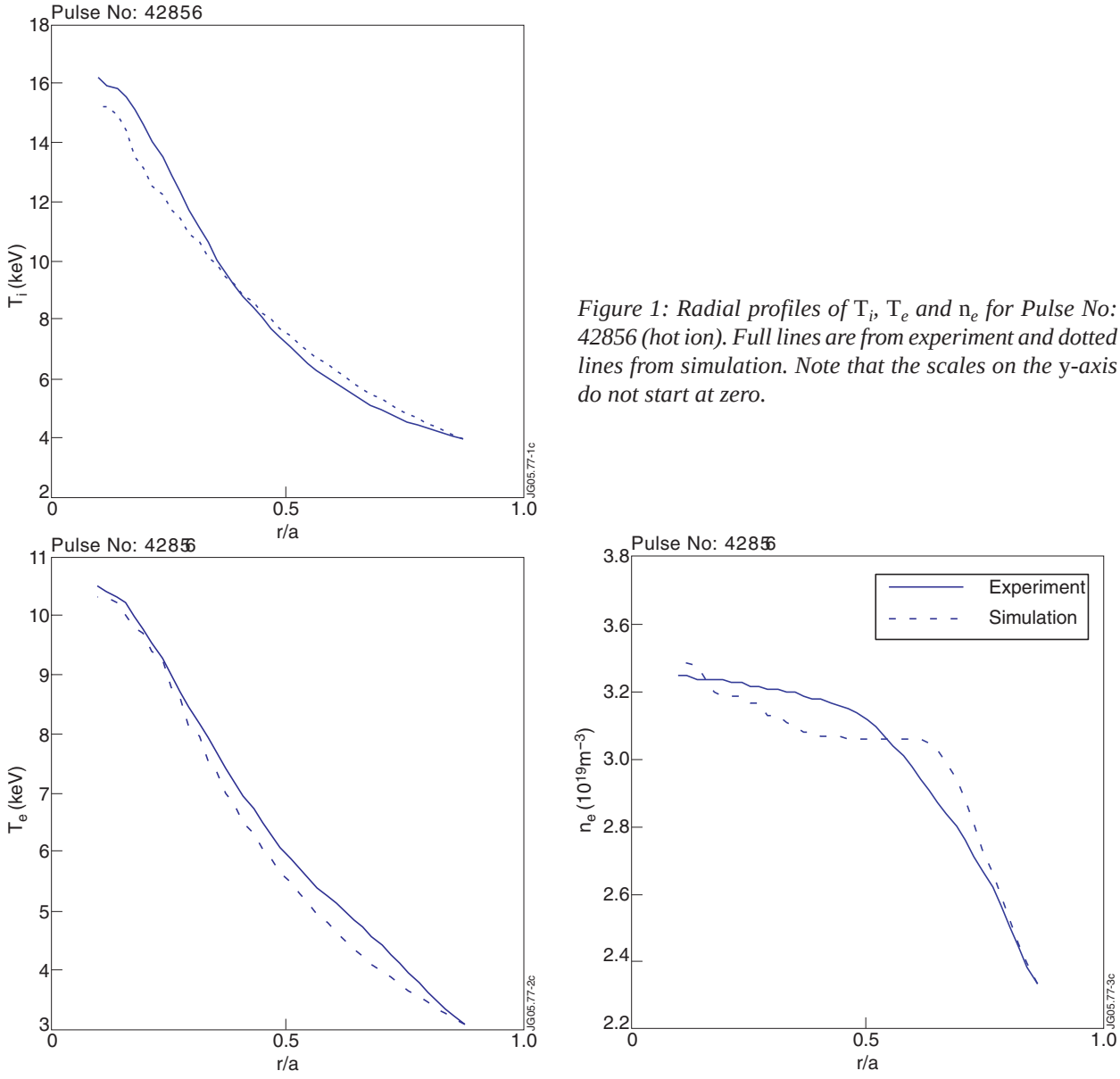

Figure 1: Radial profiles of T_i, T_e *and* n_e *for Pulse No: 42856 (hot ion). Full lines are from experiment and dotted lines from simulation. Note that the scales on the* y*-axis do not start at zero.*

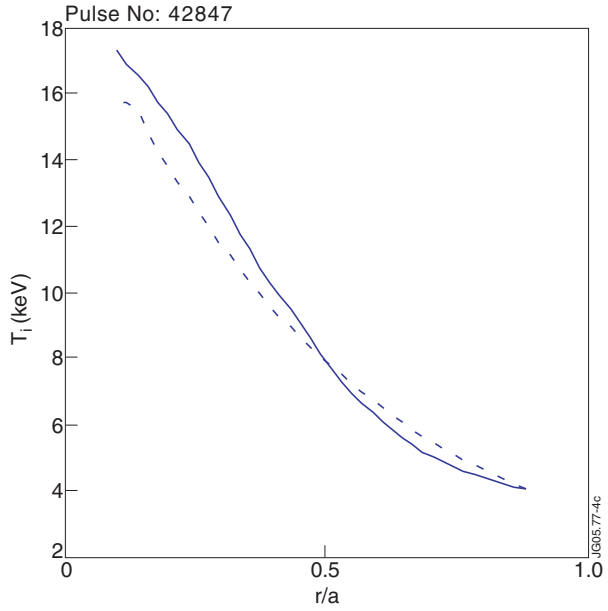

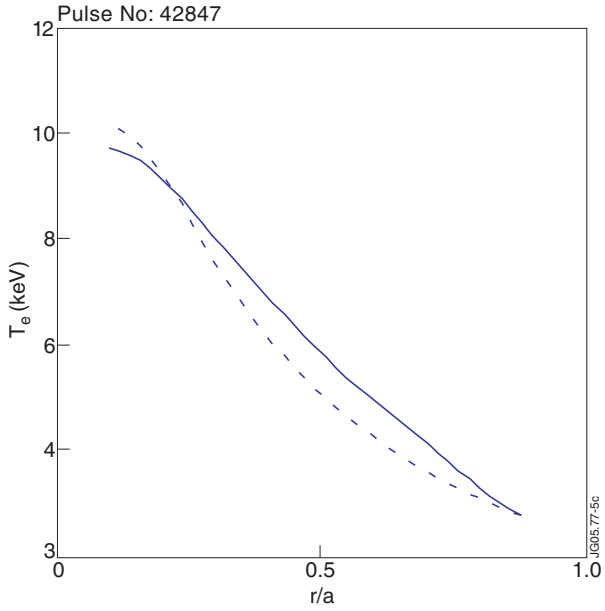

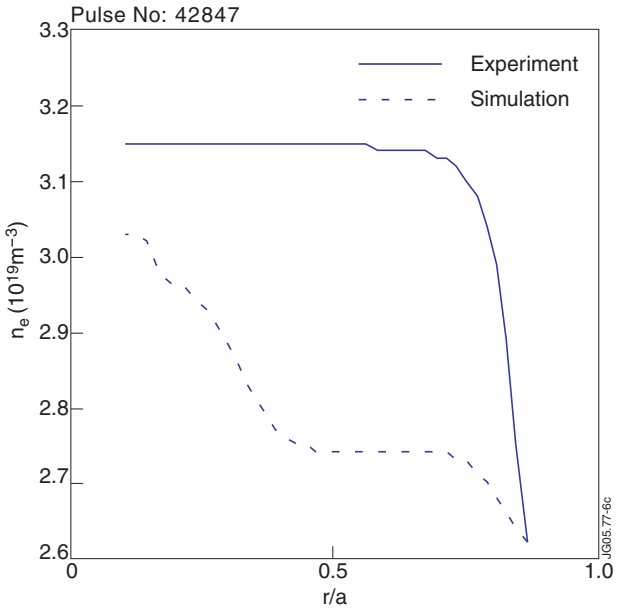

Figure 2: Simulation of Pulse No: 42847. This pulse is similar to Pulse No: 42856 but with less density peaking. The fact that the scale on the y*-axis does not start at zero here strongly magnifies the deviation in the density simulation.*

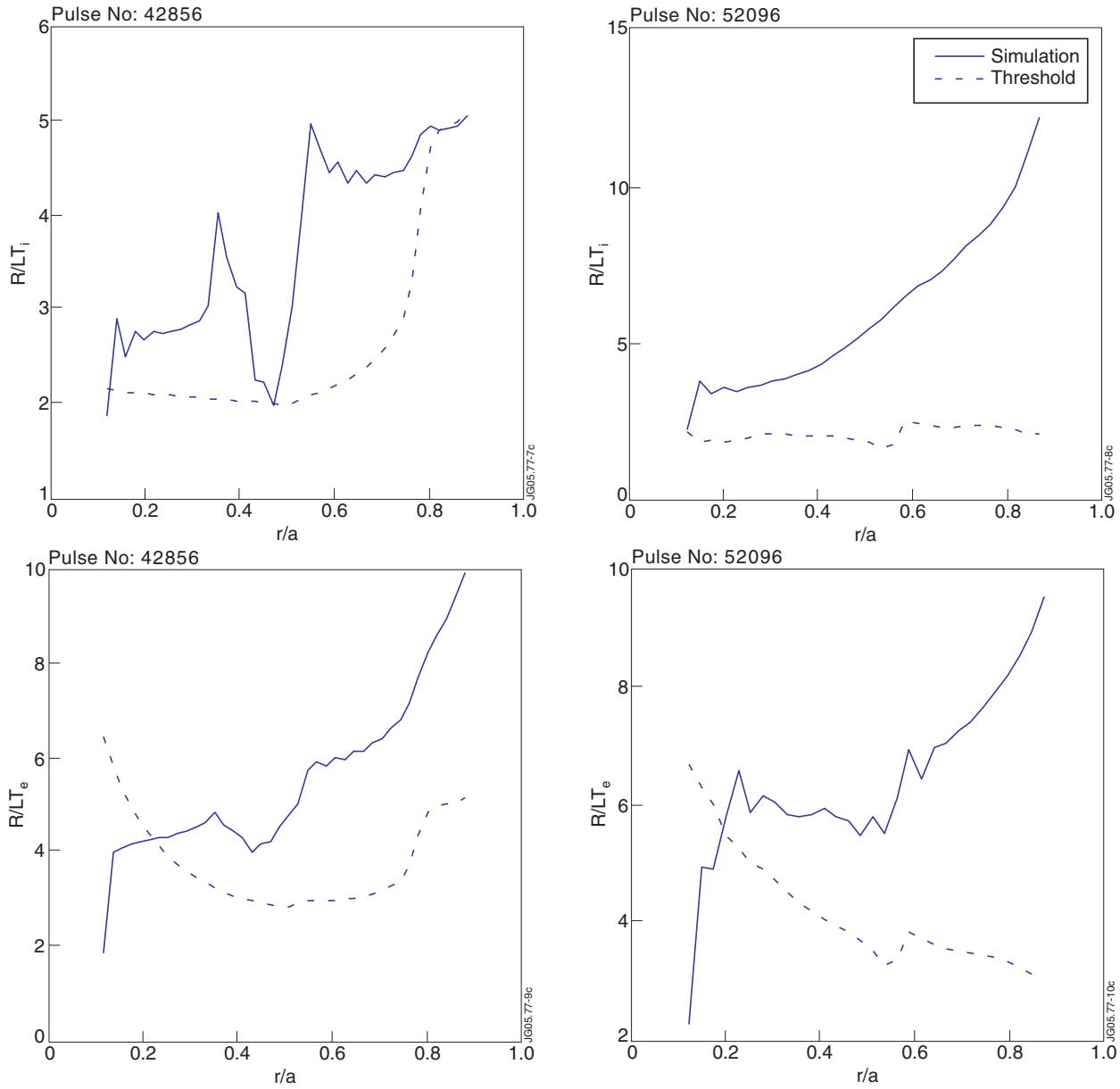

Figure 3: Radial profiles of gradients and thresholds for JET 42856 (hot ion) and JET 52096 (hot electron).

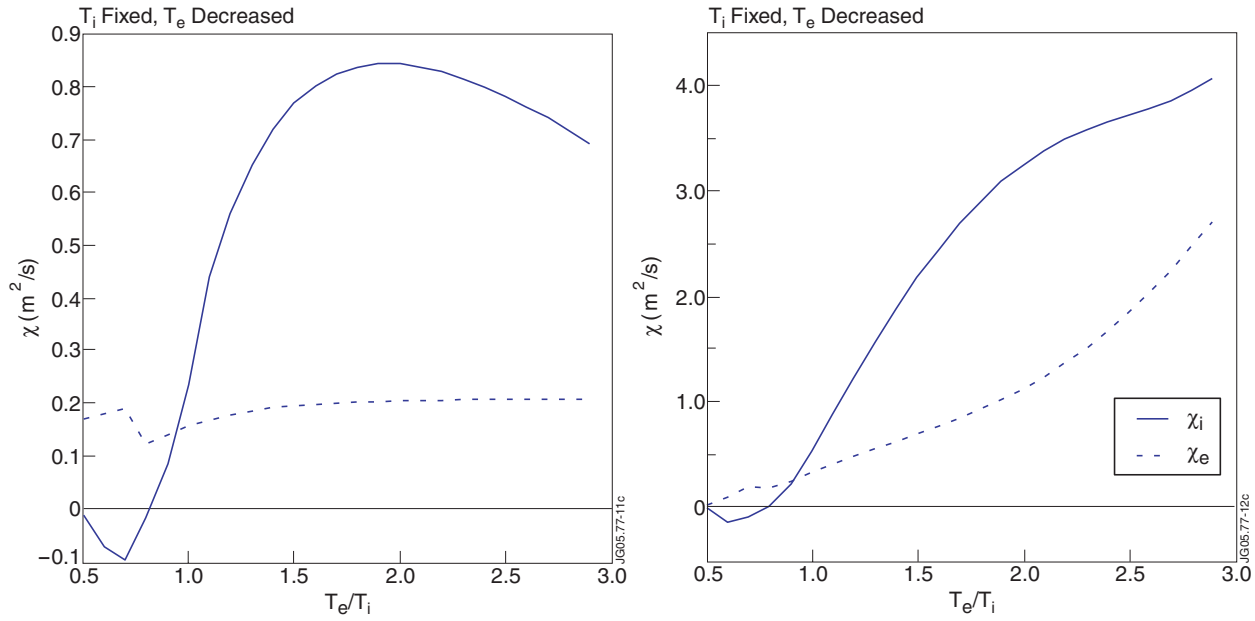

Figure 4. Ion heat pinch obtained in the hot ion regime by varying either T_i or T_e.